

## Supplementary Information

### **Band-Gap Engineering of Bi-MOFs via Anthraquinone Integration for Boosting Photocatalytic H<sub>2</sub>O<sub>2</sub> Production over a Donor-Acceptor-Acceptor Junction**

*Yunyun Gong\**, *Baihui Wang*, *Junqing Hao*, *Jianting Wang*, *Meiyu Xu*, *Mingyang Meng*, *Meichao Gao\**, *Yuanyuan Feng\**

*Key Laboratory of Catalytic Conversion and Clean Energy in Universities of Shandong Province, School of Chemistry and Chemical Engineering, Qufu Normal University, Qufu 273165 P. R. China*

*Corresponding author.*

*E-mail: [gongyunyun2013@163.com](mailto:gongyunyun2013@163.com) (Y. Gong); [meichaogao@hotmail.com](mailto:meichaogao@hotmail.com) (M. Gao); [fengyy@qfnu.edu.cn](mailto:fengyy@qfnu.edu.cn) (Y. Feng).*

## Experimental section

### 1. Material

All chemicals and reagents were of analytical grades and used without further purification. Formaldehyde (HCHO, 38%), resorcinol (C<sub>6</sub>H<sub>6</sub>O<sub>2</sub>, 99%), ammonia solution (NH<sub>3</sub>·H<sub>2</sub>O, 25~28%), absolute ethyl alcohol (C<sub>2</sub>H<sub>5</sub>OH, 99.8%), bismuth nitrate pentahydrate (Bi(NO<sub>3</sub>)<sub>3</sub>·5H<sub>2</sub>O, 99%), 1,3,5-benzenetricarboxylic acid (C<sub>9</sub>H<sub>6</sub>O<sub>6</sub>, 99%), N,N-dimethylformamide (C<sub>3</sub>H<sub>7</sub>NO, 99.9%), 1-aminoanthraquinone (C<sub>14</sub>H<sub>9</sub>NO<sub>2</sub>, 99%), isopropanol (C<sub>3</sub>H<sub>8</sub>O, 99.9%), para-benzoquinone (C<sub>6</sub>H<sub>4</sub>O<sub>2</sub>, 99%), tryptophan (C<sub>11</sub>H<sub>12</sub>N<sub>2</sub>O<sub>2</sub>, 99%), ammonium oxalate ((NH<sub>4</sub>)<sub>2</sub>C<sub>2</sub>O<sub>4</sub>, 99%), potassium iodide (KI, 99%), ammonium molybdate tetrahydrate ((NH<sub>4</sub>)<sub>6</sub>Mo<sub>7</sub>O<sub>24</sub>, 99%), potassium ferricyanide (K<sub>3</sub>[Fe(CN)<sub>6</sub>], 99%) and sodium sulfate (Na<sub>2</sub>SO<sub>4</sub>, 99%) were purchased from Shanghai Sinopharm Chemical Reagent Co., Ltd, China.

### 2. Synthesis of Bi-MOF

The pristine Bi-MOF sample was prepared by a solvothermal method. Firstly, 750 mg of H<sub>3</sub>BTC (1,3,5-benzenetricarboxylic acid) and 150 mg of Bi(NO<sub>3</sub>)<sub>3</sub>·5H<sub>2</sub>O were dissolved in 60 mL of DMF (N, N-dimethylformamide) and ultrasonicated for 15 min. Then, the mixture was moved to a 100 mL Teflon-lined autoclave and reacted at 120°C for 24 h. The precipitate was filtered by centrifugation, washed with DMF and absolute ethanol, and finally dried at 60°C for 12 h.

### 3. Synthesis of Bi-MOF/AQ

Typically, a certain mass of AMAQ (1-aminoanthraquinone), 750 mg of H<sub>3</sub>BTC, and 150 mg of Bi(NO<sub>3</sub>)<sub>3</sub>·5H<sub>2</sub>O were dissolved in 60 mL of DMF and ultrasonic oscillation for 15 min. Then, the mixture was moved to a 100 mL Teflon-lined autoclave and heated at 120°C for 24 h. The precipitate was collected by centrifugation, washed with DMF and absolute ethanol, and then dried at 60°C for 12 h.

### 4. Synthesis of RF/Bi-MOF

A certain mass of RF was dispersed into pure DMF. Then, 750 mg of H<sub>3</sub>BTC, and 150 mg of Bi(NO<sub>3</sub>)<sub>3</sub>·5H<sub>2</sub>O were added to the mixture, followed by ultrasonication for 15 min. The resulting mixture was transferred into a 100 mL Teflon-lined autoclave and heated at 120°C for 24 h. The precipitate was collected by centrifugation, washed with DMF

and absolute ethanol, and then dried at 60°C for 12 h. The obtained products were respectively labeled as RF/BiMOF-X (X = 0.1, 0.2, 0.3 and 0.4).

## 5. Characterization

X-ray diffraction (XRD) patterns were recorded by a diffractometer (D8 Advance, Bruker Co., Germany) with Cu K $\alpha$ -irradiation operated at 40 kV and 30 mA. Fourier transform infrared spectroscopy (FTIR) spectra were recorded on a Thermo Electron Nicolet-360 instrument. Sample morphologies were observed by a JSM-6700F scanning electron microscope (SEM). Transmission electron microscopy (TEM, JEM-2100 instrument, JEOL Ltd., Japan) was performed to gain morphology and crystalline structure information of samples. X-ray photoelectron spectra (XPS) were collected by an X-ray photoelectron spectrometer (Kratos Axis Ultra). The absorption spectra and diffuse reflection spectra of samples were characterized using an ultraviolet-visible spectrophotometer (TU-1901, Beijing Puxi General Instrument). Electron paramagnetic resonance (EPR) spectra were performed on a Bruker EMXPLUS spectrometer. The photoelectrochemical property was tested using a CHI760E electrochemical workstation in Na<sub>2</sub>SO<sub>4</sub> solution (0.5 M, pH=7) with a three-electrode system: Ag/AgCl reference electrode, Pt plate counter electrode. FTO supporting photocatalyst was a working electrode and a 300 W Xenon lamp was employed as the light source.

## 6. Photocatalytic Production of H<sub>2</sub>O<sub>2</sub>

20 mg of photocatalyst was dissolved in 50 mL of deionized water and ultrasonically oscillate for 10 min. Then the solution was placed in the dark for magnetic stirring for 30 min, and then the photocatalytic reaction was carried out for 1 h under a 300 W xenon lamp simulating sunlight at room temperature. Finally, 5 mL of the solution was taken out with a syringe, and the photocatalyst was filtered and separated by an MCE filter membrane. The clear liquid after filtration was further tested. The detection of H<sub>2</sub>O<sub>2</sub> adopts the standard iodometric method. 50  $\mu$ L of 0.01 mol/L (NH<sub>4</sub>)<sub>6</sub>Mo<sub>7</sub>O<sub>24</sub> aqueous solution and 2 mL of 0.1 mol/L KI aqueous solution were added to 5 mL of filtrate, mixed evenly and then left to stand for 10 min. H<sub>2</sub>O<sub>2</sub> molecules react with iodide ions (I<sup>-</sup>) in an acidic environment to form I<sub>3</sub><sup>-</sup> anions, which exhibit strong light absorption at 352 nm. The content of I<sub>3</sub><sup>-</sup> was determined by ultraviolet-visible spectroscopy, thereby calculating the content of H<sub>2</sub>O<sub>2</sub>.

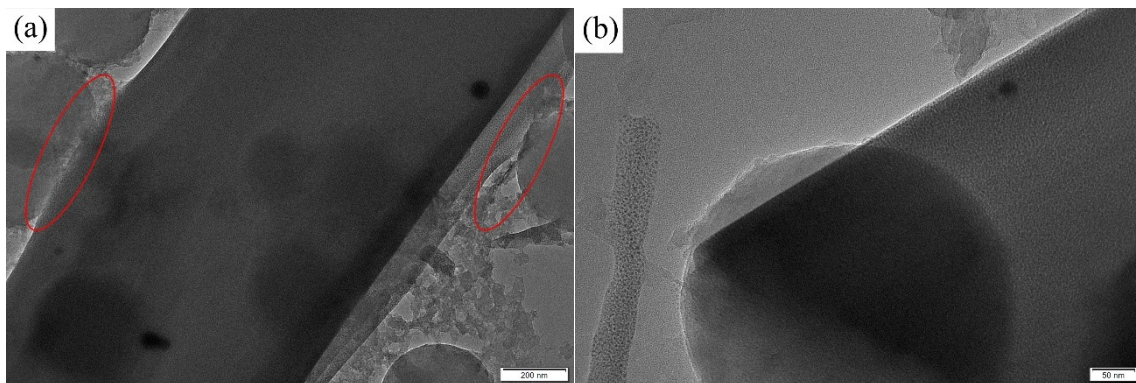


**Fig. S1.** HRTEM images of the R/B/Q-5% composite.

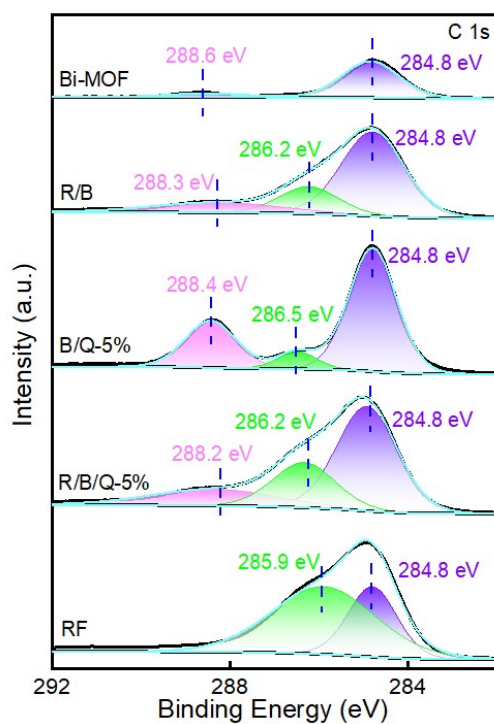


**Fig. S2.** XPS spectra of RF, R/B/Q-5%, B/Q-5%, R/B and Bi-MOF: C 1s.

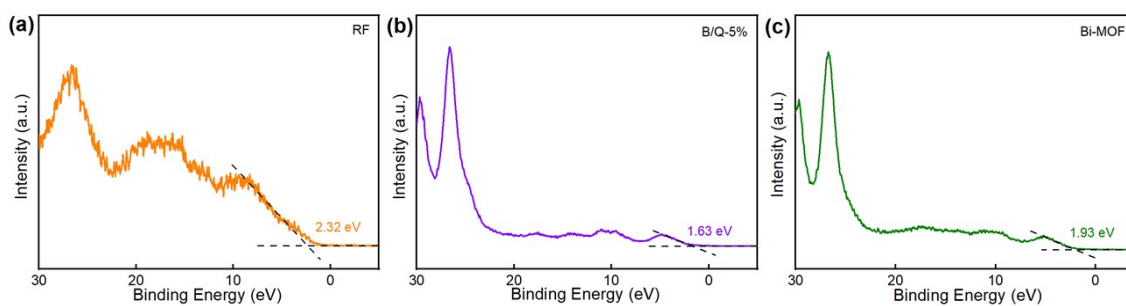


**Fig. S3.** Valence band-XPS spectrum of the (a) RF, (b) B/Q-5% and (c) Bi-MOF.

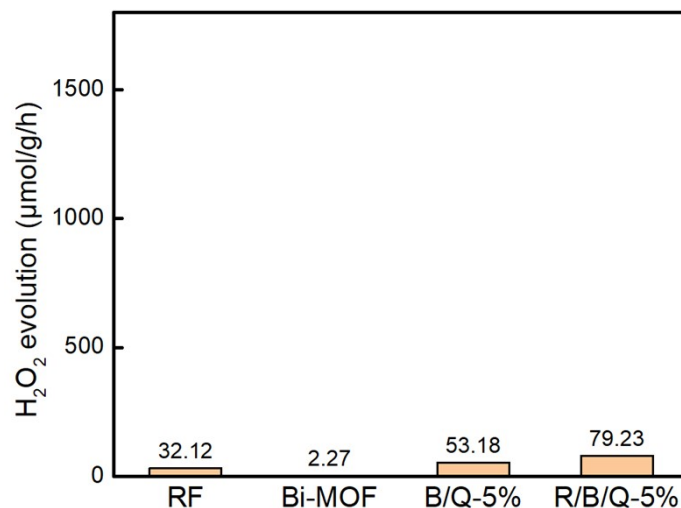


**Fig. S4.** Control experiments for the KI colorimetric assay in the dark.

Absorbance spectra at 390 nm for RF, Bi-MOF, B/Q-5%, and R/B/Q-5% dispersions in the presence of KI under dark conditions. The negligible signal confirms that the materials, including RF and AQ, do not catalytically oxidize KI or interfere with the colorimetric reaction in the absence of light, validating the photocatalytic H<sub>2</sub>O<sub>2</sub> production signals measured under illumination in Fig. S4.

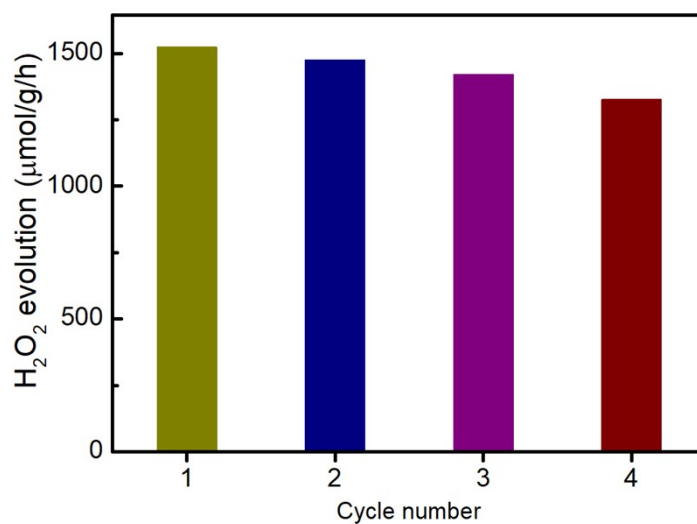


**Fig. S5.** Durability test of R/B/Q-5% in photocatalytic H<sub>2</sub>O<sub>2</sub> production.

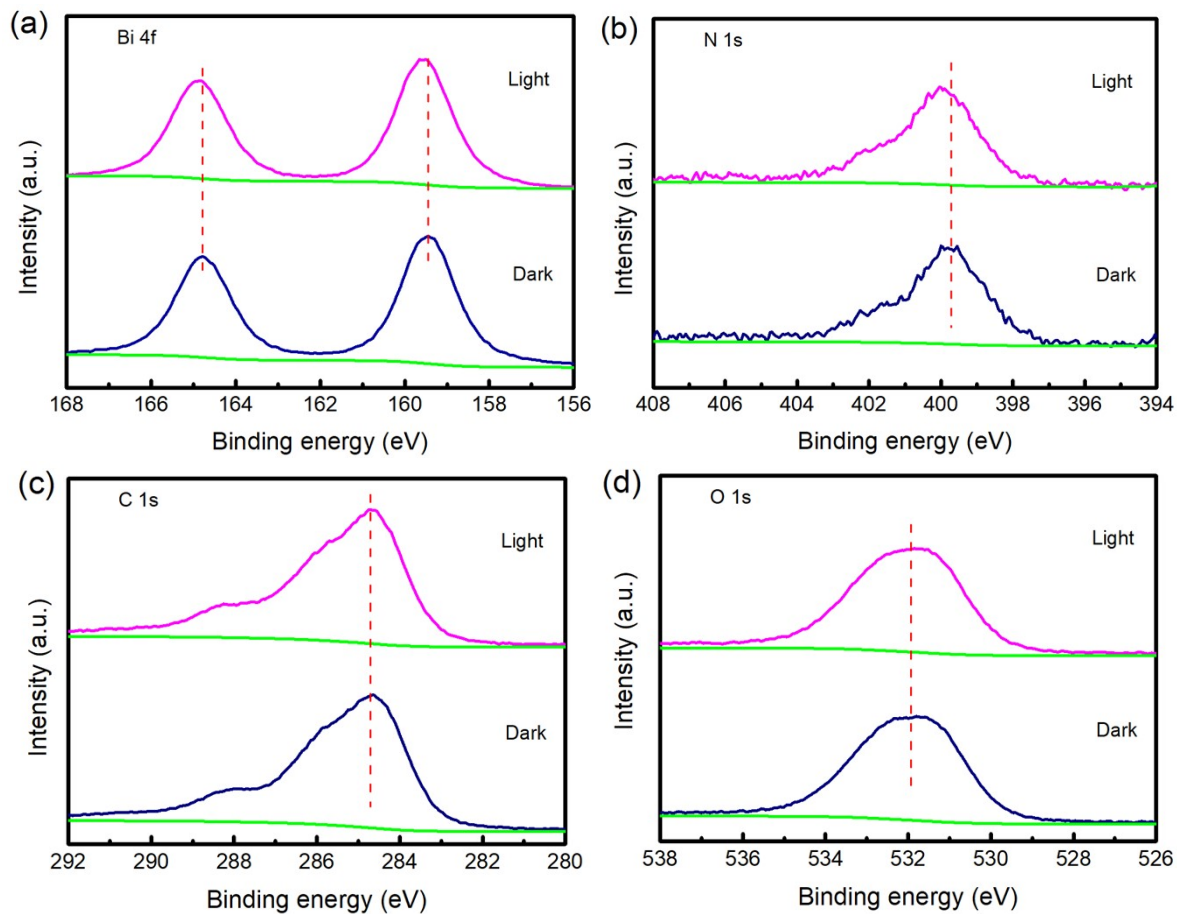


**Fig. S6.** In-situ Irradiated XPS (a) Bi 4f, (b) N 1s, (c) C 1s, (d) O 1s.

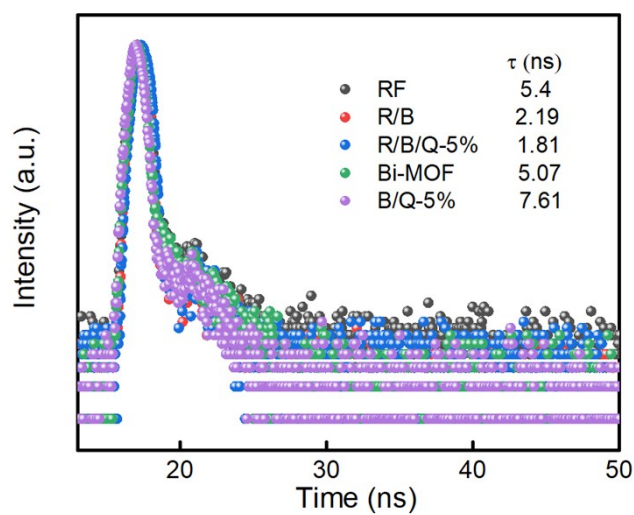


**Fig. S7.** Time-resolved fluorescence lifetime spectra of RF, R/B/Q-5%, B/Q-5%, R/B and Bi-MOF.

**Table S1.** Comparative table of performance of photocatalytic production of H<sub>2</sub>O<sub>2</sub>.

Materials	Light source (nm)	Solvent system	H <sub>2</sub> O <sub>2</sub> yield (μmol·h <sup>-1</sup> ·g <sup>-1</sup> )	Ref.
R/B/Q-5%	300 W Xe	Water	1523.25	This work
SiW <sub>11</sub> /g-C <sub>3</sub> N <sub>4</sub>	AM 1.5G	5% Methanol	152	1
PCN-NV <sub>C</sub>	λ > 420 nm	Methanol	502	2
CNK0.2	λ ≥ 420 nm	5% Methanol	1010	3
MIL-125/MIL-125-NH <sub>2</sub>	Visible	Methanol	38	4
Au/WO <sub>3</sub>	λ ≥ 420 nm	Methanol	240	5
NiO/red phosphorus	λ ≥ 420 nm	Methanol	57.3	6
NiO/CeO <sub>2</sub>	Xe light	Methanol	28.6	7
HEP-TAPB-COF	λ > 420 nm	Methanol	990	8
B/BF-750	Xe light	H <sub>2</sub> O/MeOH (9:1)	280.5	9
PTA <sub>0.6</sub> /CN	Visible light	Water	833	10
CTF-BDDBN	λ > 420 nm	Water	887	11
PDI/BCN-Ag	λ > 420 nm	Water	143	12
Reduced g-C <sub>3</sub> N <sub>4</sub> -450	λ > 420 nm	Water	170	13
ZnPPc-NBCN	Xe lamp	Water	114	14
Few-layer C <sub>60</sub>	λ > 420 nm	Water	116	15
CNOP	λ ≥ 420 nm	Water	930	16

## References

1 S. Zhao, X. Zhao, S. Ouyang, Y. Zhu, Polyoxometalates Covalently Combined with Graphitic Carbon Nitride for Photocatalytic

Hydrogen Peroxide Production, *Catal. Sci. Technol.*, 2018, **8**, 1686-1695.

2 F. Lin, T. Wang, Z. Ren, X. Cai, Y. Wang, J. Chen, J. Wang, S. Zang, F. Mao, L. Lv, Central Nitrogen Vacancies in Polymeric Carbon Nitride for Boosted Photocatalytic H<sub>2</sub>O<sub>2</sub> Production, *J. Colloid Interface Sci.*, 2023, **636**, 223-229.

3 Y. Wang, D. Meng, X. Zhao, Visible-Light-Driven H<sub>2</sub>O<sub>2</sub> Production from O<sub>2</sub> Reduction with Nitrogen Vacancy-Rich and Porous Graphitic Carbon Nitride, *Appl. Catal., B*, 2020, **273**, 119064.

4 X. Liao, W. Wei, Y. Zhou, M. Zhang, Y. Cai, H. Liu, Y. Yao, S. Lu, Q. Hao, A Ti-Based Bi-MOF for The Tandem Reaction of H<sub>2</sub>O<sub>2</sub> Generation and Catalytic Oxidative Desulfurization, *Catal. Sci. Technol.*, 2020, **10**, 1015-1022.

5 Y. Wang, Y. Wang, J. Zhao, M. Chen, X. Huang, Y. Xu, Efficient Production of H<sub>2</sub>O<sub>2</sub> on Au/WO<sub>3</sub> under Visible Light and the Influencing Factors, *Appl. Catal., B*, 2021, **284**, 119691.

6 N. Chen, J. Cao, M. Guo, C. Liu, H. Lin, S. Chen, Novel NiO/RP Composite with Remarkably Enhanced Photocatalytic Activity for H<sub>2</sub> Evolution from Water, *Int. J. Hydrogen Energy*, 2021, **46**, 19363-19372.

7 P. Li, M. Zhang, X. Li, C. Wang, R. Wang, B. Wang, H. Yan, MOF-Derived NiO/CeO<sub>2</sub> Heterojunction: A Photocatalyst for Degrading Pollutants and Hydrogen Evolution, *J. Mater. Sci.*, 2020, **55**, 15930-15944.

8 D. Chen, W. Chen, Y. Wu, L. Wang, X. Wu, H. Xu, L. Chen, Covalent Organic Frameworks Containing Dual O<sub>2</sub> Reduction Centers for Overall Photosynthetic Hydrogen Peroxide Production, *Angew. Chem. Int. Ed.*, 2023, **62**, e202217479.

9 J. Wang, Y. Gong, M. Gao, Y. Zheng, Y. Feng, M. Xu, Q. Chu, J. Yan, Bi<sub>2</sub>O<sub>2</sub>CO<sub>3</sub> Nanosheet Composites with Bi-Based Metal-Organic Frameworks for Photocatalytic H<sub>2</sub>O<sub>2</sub> Production, *ACS Appl. Nano Mater.*, 2024, **7**, 1067-1077.

10 J. Cao, Q. Wu, Y. Zhao, K. Wei, Y. Li, X. Wang, F. Liao, H. Huang, M. Shao, Y. Liu, Z. Kang, In-Situ Photovoltage Transients Assisted Catalytic Study on H<sub>2</sub>O<sub>2</sub> Photoproduction over Organic Molecules Modified Carbon Nitride Photocatalyst, *Appl. Catal., B*, 2021, **285**, 119817.

11 L. Chen, L. Wang, Y.Y. Wan, Y. Zhang, Z.M. Qi, X.J. Wu, H.X. Xu, Acetylene and Diacetylene Functionalized Covalent Triazine Frameworks as Metal-Free Photocatalysts for Hydrogen Peroxide Production: A New Two-Electron Water Oxidation Pathway, *Adv. Mater.*, 2020, **32**, 1904433.

12 P. Liu, T. Liang, J. Bian, Z. Li, Z. Zhang, L. Jing, Improved Photocatalytic H<sub>2</sub>O<sub>2</sub> Production of Boron Doped g-C<sub>3</sub>N<sub>4</sub> by Controllably Co-Modifying Nanosized PDI and Ag, *Mater. Res. Bull.*, 2023, **167**, 112370.

13 Z. Zhu, H. Pan, M. Murugananthan, J. Gong, Y. Zhang, Visible Light-Driven Photocatalytically Active g-C<sub>3</sub>N<sub>4</sub> Material for Enhanced Generation of H<sub>2</sub>O<sub>2</sub>, *Appl. Catal., B*, 2018, **232**, 19-25.

14 Y.-X. Ye, J. Pan, F. Xie, L. Gong, S. Huang, Z. Ke, F. Zhu, J. Xu, G. Ouyang, Highly Efficient Photosynthesis of Hydrogen Peroxide in Ambient Conditions, *PNAS*, 2021, **118**, e2103964118.

15 T.T. Wang, L. Zhang, J.B. Wu, M.Q. Chen, S.F. Yang, Y.L. Lu, P.W. Du, Few-Layer Fullerene Network for Photocatalytic Pure Water Splitting into H<sub>2</sub> and H<sub>2</sub>O<sub>2</sub>, *Angew. Chem. Int. Ed.*, 2023, **62**, e202311352.

16 H. Kim, K. Shim, K.E. Lee, J.W. Han, Y. Zhu, W. Choi, Photocatalytic Production of H<sub>2</sub>O<sub>2</sub> from Water and Dioxygen Only under Visible Light Using Organic Polymers: Systematic Study of the Effects of Heteroatoms, *Appl. Catal., B*, 2021, **299**, 120666.